A mechanism-based model for the population pharmacokinetics of free and bound aflibercept in healthy subjects.

Hoai-Thu Thai, Christine Veyrat-Follet, Nicole Vivier, Catherine Dubruc, Gérard Sanderink, France Mentré, Emmanuelle Comets

▶ **To cite this version:**

A mechanism-based model for the population pharmacokinetics of free and bound aflibercept in healthy subjects

Hoai-Thu Thai[1,2], Christine Veyrat-Follet[1], Nicole Vivier[1], Catherine Dubruc[1], Gerard Sanderink[1], France Mentré[2], Emmanuelle Comets[2]

[1] Global Metabolism and Pharmacokinetics Department, Sanofi-aventis, Paris, France

[2] UMR738, INSERM, University Paris Diderot, Paris, France

Correspondence:

Hoai-Thu Thai

UMR738, INSERM, University Paris Diderot

16 rue Henri-Huchard

75018 Paris, France

Tel: + 33 1 57 27 75 38

Email: hoai-thu.thai@inserm.fr

Keywords: Population pharmacokinetics, target-mediated drug disposition, aflibercept, VEGF, MONOLIX

Running head: Population PK model of aflibercept

Word count: title (115 characters including spaces), summary (185 words), content (4411 words)

Number of tables: 1

Number of figures: 5

"What this paper adds" statement

What is already known about this subject

Anti-angiogenic drugs have been developed as an effective therapeutic strategy for inhibiting tumour growth. However, their pharmacokinetics (PK) and their ligand inhibition properties have not been well characterised. The binding to a circulating target, such as vascular endothelial growth factor (VEGF), makes the PK of these drugs more complex.

What this study adds

The underlying mechanism of disposition of aflibercept, where a saturable and high-affinity binding of aflibercept to VEGF was adequately characterised by the Michaelis-Menten approximation of a target-mediated drug distribution (TMDD) model. To our knowledge, it is the first published mechanism-based population pharmacokinetic model for an anti-VEGF drug.

Summary

Aim: Aflibercept (VEGF-Trap), a novel antiangiogenic agent that binds to VEGF, has been investigated for the treatment of cancer. The aim of this study was to develop a mechanism-based pharmacokinetic model for aflibercept to characterise its binding to VEGF and its pharmacokinetic properties in healthy subjects.

Methods: Data from two phase I clinical studies with aflibercept administered as a single intravenous infusion were included in the analysis. Free and bound aflibercept concentration-time data were analyzed using a nonlinear mixed-effects modelling approach with MONOLIX 3.1.

Results: The best structural model involves two compartments for free aflibercept and one for bound aflibercept, with a Michaelis-Menten type binding of free aflibercept to VEGF from the peripheral compartment. The typical estimated clearances for free and bound aflibercept were 0.88 L/day and 0.14 L/day, respectively. The central volume of distribution of free aflibercept was 4.94 L. The maximum binding capacity was 0.99 mg/day and the concentration of aflibercept corresponding to half of maximum binding capacity was 2.91 µg/mL. Interindividual variability of model parameters was moderate, ranging from 13.6 % (V_{max}) to 49.8 % (Q).

Conclusion: The present PK model for aflibercept adequately characterises the underlying mechanism of disposition of aflibercept and its nonlinear binding to VEGF.

Introduction

Angiogenesis, the development of new blood vessels from pre-existing vasculature, participates in a variety of physiological processes and disease states [1]. Its critical role in tumour development and progression was established 30 years ago [2]. This discovery brought a new effective approach called anti-angiogenic therapy to cancer treatment, which consists in limiting blood supply to tumours by preventing angiogenesis. The development of new agents has attracted many researchers' interest in the pharmaceutical industry. To date, the best characterised and most highly validated anti-angiogenic approach involves targeting the vascular endothelial growth factor (VEGF) pathway [3].

VEGF is the most potent pro-angiogenic growth factor, promoting the formation of blood vessels which is required for both normal and neoplastic tissue growth [1, 4]. VEGF binds to two high-affinity receptors (VEGFR-1 and VEGFR-2) on endothelial cells. This binding activates the intrinsic tyrosine kinase activity of their cytodomains, initiating intracellular signalling. VEGF is expressed in a large variety of malignant tumours, such as tumours of breast, brain, lung and gastrointestinal tract [5]. Blockade of VEGF pathway is therefore an effective therapeutic strategy for inhibiting tumour growth [4-6].

Aflibercept (also called VEGF-Trap, Regeneron Pharmaceutics/ Sanofi-aventis research) is a novel anti-angiogenic agent that binds to VEGF with a 1:1 ratio and prevents it from interacting with its receptors. A recombinant fusion protein consisting of the second Ig domain of VEGFR-1 and the third Ig domain of VEGFR-2 fused to the Fc portion of human immunoglobin IgG1, it has a higher affinity for VEGF-A (K_d *in vitro* = 0.5 pM) than current anti-VEGF monoclonal

antibodies [7-9]. Aflibercept also binds to VEGF-B and Placental Growth Factor (PlGF), which may be advantageous in some settings, such as malignant ascites where PlGF may mediate vascular permeability [9].

Based on the mechanism of action, this drug undergoes a target-mediated drug disposition (TMDD), a term used to describe the phenomenon in which drug is bound with high affinity to its pharmacologic target such that this interaction is reflected in the pharmacokinetic properties of the drug. A general PK model for drugs exhibiting TMDD has been developed by Mager et al [10, 11]. This model describes the elimination pathway of drug plasma concentrations as the combination of first-order elimination from the central compartment and specific target binding clearance followed by internalization of drug-target complex. It, as well, characterises the turnover of the target. The full TMDD model is complex and generally overparameterised. The more information we have about free drug, bound drug and the target, the more TMDD model components and parameters can be adequately identified, although it is yet unclear which elements should be measured to estimate all the parameters in the full TMDD model. In order to overcome this problem, several simpler forms of TMDD model were proposed [12, 13]. There are mainly three approximations: quasi equilibrium (QE), quasi steady state (QSS) and Michaelis-Menten (MM). The QE approximation is based on the assumption that the drug-target binding is much faster than all other system processes. If the rate of elimination of complex is not negligible, the QE approximation is replaced by the QSS approximation assuming that the drug-target complex concentration changes more showly than the binding and internalization process. The MM approximation describes the system when the target concentration is small relative to the free drug concentration and the dosing regimens result in the target being fully saturated [13].

Pharmacokinetics (PK) of aflibercept were investigated in healthy subjects after single intravenous (i.v.) doses of 1 to 4 mg/kg and single subcutaneous (s.c.) dose of 2 mg/kg, in two phase I clinical studies as part of the drug's clinical development. Both free and bound aflibercept concentrations were assayed. The objective of this analysis was to develop a mechanism-based PK model for aflibercept in order to characterise its binding to VEGF and its pharmacokinetic properties in healthy subjects. The influence of covariate was not assessed in this study due to the limited number of individuals and their healthy status

Methods

Study design

The data for the population PK analysis were collected from two phase I, monocentric and randomised studies which were both carried out in healthy male subjects to assess the PK of aflibercept. The studies were approved by the independent ethics committees (Pharma-Ethics, South Africa and Ethik-Kommission der Landesärztekammer Baden-Württemberg, Germany). They are performed according to recommendations of the 18th World Health Congress (Helsinki, 1964) and all applicable amendments. The volunteers gave their written informed consent after full explanation of all procedures involved in the studies.

Study 1 was a placebo-controlled, single-dose, sequential ascending dose study. Forty eight subjects were enrolled in this study and equally divided into four groups: one group receiving placebo and three groups receiving a single dose of 1, 2 or 4 mg/kg of aflibercept respectively administered as a 1-hour i.v. infusion.

Study 2 was an open-label, single-dose, crossover study. Two groups of 20 subjects were included in the study. The first group received a single i.v. dose of 2 mg/kg in the first period, with a 2 month follow-up period, followed by a single s.c. dose of 2 mg/kg in the second period. The second group received the s.c. dose first, then the i.v. dose.

The data from subcutaneous administration in the cross-over study (study 2) was removed from the analysis because this route of administration was not pursued in the subsequent clinical development. Moreover, in this study, a carry-over effect was found and should have been taken into account in the modelling, but this required the modelling of the subcutaneous route. To avoid it and to work on homogenous data, only the i.v. infusion data in the first period were used in the population analysis.

Blood sampling schedules

In study 1, blood samples (4 mL) were taken at the following times: predose, 1 (end of infusion), 2, 4, 6, 8, 12, 24 hours post-start of administration on day 1, then on days 8, 15, 22, 29, 36 and 43 at the same morning time corresponding to 2 hours after the start of infusion on day 1.

In study 2, blood samples (4 mL) were taken at the following times: predose, 1, 2, 4, 6, 8 hours post-start of administration on day 1, then on days 2, 3, 5, 8, 15, 29, 43 of each period at the same morning time corresponding to 2 hours after the start of infusion on day 1.

Assay method

For both studies, free and bound aflibercept plasma concentrations were measured in all samples collected collected at Regeneron Pharmaceuticals, Inc using enzyme-linked immunosorbent assay (Elisa) method. Blood samples were collected in tubes (containing 1mL of citrate buffer, sodium

citrate, and 4.2 mg of citric acid) and were centrifuged at 2000 g for 15 minutes at room temperature. Plasma was stored at -20°C until analyzed.

In the assay of free aflibercept, the human VEGF165 was initially adsorbed to the surface of a polystyrene solid support to capture the free aflibercept in subject samples. A mouse monoclonal antibody (reporter antibody), specific to an epitope on the VEGFR1 domain of aflibercept, was then bound to the immobilized complex and an enzyme-linkedantibody (peroxidase-conjugated Affinipure goat anti-mouse IgG Fc-γ) was bound to the immobilized mouse monoclonal complex. A luminolbased substrate specific for peroxidase was added to achieve a signal intensity that was directly proportional to the concentration of free aflibercept. The limit of quantification of free aflibercept was 15.6 ng/mL. The calibration curves ranges from 100 ng/mL to 1.56 ng/mL in two-fold serial dilution. The limit of quantification of free aflibercept was 15.6 ng/mL. The inter-day accuracy and precision ranged from 92.24% to 103.09% and 1.05% to 16.18%, respectively. The intra-day accuracy and precision ranged from 106.36% to 109.90% and 9.56% to 13.68%, respectively.

In the assay of bound aflibercept, the human VEGF165 was replaced by a non-blocking goat anti-human VEGF antibody for capturing the bound aflibercept in subject samples. The rest of the procedure was similar as the one used in the assay of free aflibercept. The limit of quantification for bound aflibercept is 43.9 ng/mL. The calibration curves ranges from 100 ng/mL to 8.78 ng/mL in a 1.5 serial dilution. The inter-day accuracy and precision ranged from 93.85% to 110.19 % and 0.38% to 16.17%, respectively. The intra-day accuracy and precision ranged from 115.70% to 123.34% and 1.09% to 1.58%, respectively.

Population PK analysis

The population PK analysis was performed using the MONOLIX program (version 3.1) implementing the SAEM algorithm. The model control files were written using MLXTRAN script. The early concentrations of bound aflibercept were often below the limit of quantification, thus the censored data of bound aflibercept, representing 32.5% of data, were taken into account and used for model development using the extended SAEM algorithm implemented in MONOLIX as an exact maximum likelihood estimation method [14]. In this algorithm, the left-censored data are simulated in a right-truncated Gaussian distribution, instead of being imputed by the LOQ value or half of LOQ value. The data of bound aflibercept contains also some observed concentrations which were reported with values below the LOQ reported for most of the data (see bottom left plot in figure 4).

The database included a total of 56 subjects, with 36 subjects receiving treatments from study 1 and 20 subjects receiving i.v. infusions at the first period from study 2. With respect to the law of mass action, the concentrations of bound aflibercept were converted into equivalent concentrations of free aflibercept by multiplying them with 0.717, the ratio of molecular weights between free and bound aflibercept. The units of free aflibercept and bound aflibercept concentrations were µg/mL and µg.eq/mL respectively.

PK structural model

The following strategy was used to develop the model. Free aflibercept concentration-time data were first modelled alone. Then, bound concentration-time data were included for simultaneous modelling.

The structural model for free aflibercept was developed by testing the following models: two-compartment or three-compartment model with first order and/or MM elimination.

9

In the next step, we developed a structural model including bound aflibercept. The TMDD model with association and dissociation rate constants (k_{on} and k_{off}), reduced approximate TMDD models and other simpler models with linear binding constant were used to describe the joint evolution of the two entities.

Statistical model

Denoting f the function describing the model, the statistical model for observed concentration C_{ij} of subjects i for sampling time t_{ij} is:

$$C_{ij} = f(\theta_i, t_{ij}) + \varepsilon_{ij}$$

where θ_i is the vector of parameters of subject i and ε_{ij} is the residual error.

The errors ε_{ij} are assumed to be independent and normally distributed with a null mean and a heteroscedastic variance σ^2_{ij}, which was modelled using a combined additive and proportional model:

$$\sigma^2_{ij} = (\sigma_a + \sigma_p \, f(\theta_i, t_{ij}) \,)^2$$

where σ_a and σ_p are additive and proportional coefficients of residual error model respectively.

Two alternative residual error models, proportional model ($\sigma_a = 0$) and additive model ($\sigma_p = 0$) were also evaluated for the residual variability.

The interindividual variability on all parameters was modelled with an exponential model, e.g. for *CL*:

$$CL_i = CL.\exp(\eta_{i,CL})$$

10

where $\eta_{i,CL}$ denotes the random effect in subject i, CL_i the individual clearance parameter and *CL* the typical value of the population. The use of an exponential model implies a log-normal distribution for the parameters. The η's (e.g. $\eta_{i,CL}$) are zero mean random variables with variance ω^2 (e.g. for *CL*, $\omega^2 CL$). The ω^2's represent the variance of the random effects; the elements of the interindividual variance-covariance matrix, Ω, was modelled as diagonal, e.g. assuming no covariance between the η's.

The following strategy was used for model development. First, the structural PK models were developed with a combined residual error model and interindividual variability on all parameters. Then, the residual error models were evaluated for the selected structural model. Finally, the interindividual variability on each parameter was tested for significance, and non-significant variability component were removed one by one starting with the smallest and least significant estimate.

The log likelihood (LL) was computed using importance sampling. The likelihood ratio test was used to discriminate between nested models through the difference in log likelihood (-2LL). A p-value of 0.05 was considered statistically significant. For non-nested models, the model selection was based on the Bayesian information criterion BIC. The better model is the one with a smaller value of BIC [15].

Model evaluation

Internal evaluation of the model was based on goodness-of-fit (GOF) plots, including plots of observations versus individual and population predictions and plots of normalised prediction

distribution error (NPDE) [16]. A visual predictive check (VPC) was used to assess model predictive performance, based on the simulation of 500 datasets.

Results

Data

The database for population PK analysis contained data from 56 healthy subjects involved in the two phase I clinical studies. A total of 1476 concentrations were used for model building: 732 concentrations of free aflibercept and 744 concentrations of bound aflibercept of which 242 (32.5 %) were below the quantification limit (LOQ= 43.9 ng/mL or 0.0314 µg.eq/mL).

The pooled concentrations of free aflibercept and bound aflibercept plotted versus time are presented in Figure 1.

The time-course of free aflibercept after i.v. infusion of doses of 1, 2 and 4 mg/kg in semi-log scale suggests a bi-exponential decline with a rapid phase of distribution followed by a prolonged terminal phase of elimination regardless of the dose. The time-course of bound aflibercept suggests a saturable binding phenomenon with the same observed plateau for two higher doses. The peaks of complex occurred sooner for dose 1 mg/kg and later for doses 2 and 4 mg/kg (around 21 days, for both doses).

Free aflibercept modelling

Several models were proposed to characterise the kinetics of free aflibercept. In the two-compartment model with first-order elimination, the distribution of post-hoc clearance for 3 doses showed a dose-dependent clearance, confirming the nonlinear disposition already observed during

12

non-compartmental analysis. The two-compartment model with MM elimination was then developed and showed a better description of data with a decrease of 33.61 point in -2LL value. The three-compartment models with first-order or MM elimination were also evaluated. They provided a slight decrease in -2LL compared to the two-compartment models but the fitting did not show a significant improvement. The two-compartment model with MM elimination was therefore selected as an adequate structural model for free aflibercept.

The best residual error for this model was the combined additive and proportional error. The interindividual variability on K_m was not significant.

Free and bound aflibercept modelling

The binding of aflibercept to VEGF and the nonlinear kinetics of free aflibercept suggests that this drug has target-mediated drug disposition properties. Therefore, the TMDD model with association and dissociation rate constants (k_{on} and k_{off}), reduced approximate TMDD models and other simpler models with linear binding constant were tested. The MM approximation of TMDD model developed by Gibiansky and colleagues [13] was found the best approach to describe the kinetics of both free and bound aflibercept, while others did not fit the concentrations of bound correctly and/or had overparameterization issues. In all of these models, the dissociation rate k_{off} was very small compared to other constants and very badly estimated.

The nonlinear central and peripheral binding of this MM approximate TMDD model were tested and compared. The nonlinear peripheral binding model was found to better describe the data than the central binding one with a smaller value of BIC (2160 vs 2703) and therefore retained as the structural model for free and bound aflibercept.

13

The final structural model relating free and bound aflibercept is shown in Figure 2.

Free aflibercept in plasma distributes first to tissues then binds to VEGF to form the complex. Binding to VEGF follows the law of mass action and can be characterised by a nonlinear form with MM constants (V_{max}, K_m). The bound aflibercept (complex) is assumed to be directly eliminated through internalisation (k_{int}) and not through the dissociation rate constant (k_{off}) which gives back free aflibercept and free VEGF. The concentration of free aflibercept in central compartment (C_p), in tissue compartment (C_t) and the concentration of bound aflibercept (C_b) are described by means of differential equations:

$$\frac{dC_p}{dt} = Input - (k_{el} + k_{pt}).C_p + k_{tp}.\frac{C_t.V_t}{V_p} \qquad (1)$$

$$\frac{dC_t}{dt} = k_{pt}.\frac{C_p.V_p}{V_t} - k_{tp}.C_t - \frac{1}{V_t}.\frac{V_{max}.C_t}{K_m + C_t} \qquad (2)$$

$$\frac{dC_b}{dt} = \frac{1}{V_b}.\frac{V_{max}.C_t}{K_m + C_t} - k_{int}.C_b \qquad (3)$$

in which k_{el} is the first order elimination rate constant of free aflibercept (day^{-1}) from central compartment, k_{tp} and k_{pt} are the first order rate constants between central and peripheral compartment (day^{-1}), k_{int} is the first order rate constant of bound aflibercept internalization (day^{-1}), V_{max} is the maximum binding capacity (mg/day), K_m is the concentration of free aflibercept corresponding to half of maximum binding capacity (µg/mL), V_p is the central volume of distribution of free aflibercept (L), V_t is the peripheral volume of distribution of free aflibercept and V_b is the volume of distribution of bound aflibercept (L). More details concerning the derivation of the model equations and its relationship to other TMDD models proposed in the literature can be found in the Appendix.

In this model, the volume of bound aflibercept (V_b) and the maximum binding capacity (V_{max}) were however highly correlated with a correlation coefficient higher than 0.95, suggesting identifiability issues. In order to prevent this problem, the value of V_b was assumed to be equal to the value of central volume of distribution of free aflibercept (V_p), corresponding to the hypothesis that free and bound aflibercept are distributed within the same space in the plasma compartment. To do so, V_b was fixed to the population value of V_p with no interindividual variability, instead of being estimated.

The best residual error model of bound aflibercept was the proportional model, while that of free aflibercept was the combined additive and proportional error model found in the first step. A combined error model was also attempted; however, the contribution of the additive error was negligible and was therefore discarded. The interindividual variability on the internalization rate constant (k_{int}) was found to be small (11.9%) and badly estimated. The likelihood ratio test demonstrated that removing this variability from the model did not significantly change the fit.

The estimated parameter values for the best model of free and bound aflibercept are presented in Table 1.

All model parameters were well estimated with relative standard errors (RSE) < 20%. The population estimate of clearance for free aflibercept was 0.88 L/day and internalisation rate for bound aflibercept was 0.028 day^{-1}, resulting in a clearance of 0.14 L/day. The central volume of distribution for free aflibercept was 4.94 L. The maximum binding capacity was 0.99 mg/day and the estimated concentration of free aflibercept corresponding to half of maximum binding capacity was low (2.91 µg/mL).

Interindividual variability for random effects associated with model parameters was moderate, ranging from 13.6 % (V_{max}) to 49.8 % (Q). Residual errors were low for both free aflibercept and bound aflibercept with proportional parts of 17.1 % and 12.6 % respectively. The additive error of free aflibercept was also small compared to the observed concentrations.

The goodness-of-fit plots of the best joint model are shown in Figure 3. The plots of observations versus population predictions and observations versus individual predictions indicated that the model adequately described the observations over the dose range. The normalised prediction distribution error plots, NPDE versus time and NPDE versus predictions, show a symmetric distribution around zero, except for the early times and the small concentrations of bound aflibercept. This bias was caused by omitting the NPDE corresponding to below the quantification limit (BQL) observations. For BQL data, the metric NPDE has not yet been developed.

The total number of BQL concentrations of bound aflibercept predicted by the model was 251 (33.73%), 231 of which correspond to observed BQL data. This shows the good agreement between model prediction and observation for BQL data.

Examples of individual fits taken from two studies with three doses are shown in Figure 4. The model describes the observed concentrations of free and bound aflibercept for all subjects quite well.

Figure 5 presents the visual predictive checks for both free and bound aflibercept. The 80% prediction interval and median were obtained by simulating 500 datasets under the final model; in addition, we obtained the 90% prediction intervals around the median and the upper and lower boundaries of the interval. Concentrations lower than the LOQ simulated for free aflibercept at

the end of treatment were replaced by the LOQ (0.0156 µg/mL) in order to obtain a lower limit for the VPC plots in semi-logarithmic scale. The slight misfit for free aflibercept seen at the last time-point may be a consequence of the number of concentrations near the LOQ, since the median and upper boundary appear to be very well predicted by the model. For bound aflibercept, the model slightly underpredicted median concentration from day 21 onwards but correctly predicted the variability. Thus, the model described reasonably well the observed concentrations of both free and bound aflibercept.

Discussion

In this study, we report the development of a mechanism-based model to characterise the population PK of aflibercept after a single i.v. infusion of a 2 to 4 mg/kg dose to 56 healthy subjects. Free and bound aflibercept plasma concentrations were used in the modelling.

We first modelled free aflibercept concentrations alone. Using standard compartmental PK models, we observed a decrease of clearance for higher concentrations. This is consistent with previous results from noncompartemental analyses, which demonstrated that the volume of distribution of free aflibercept was low and its clearance was dose-dependent. When dealing with saturable kinetics, the most common model to consider is MM elimination kinetics, which was retained as the final model for free aflibercept during model development. Although such a model has been successfully applied to describe nonlinear PK of free aflibercept, it does not well represent the underlying molecular events such as target binding, internalization and degradation of the drug. However, the modelling of free aflibercept helped us get general information about the model structure: two compartment kinetics and dose-dependent clearance. More complex models combining linear and nonlinear elimination were also tested. They adequately fitted the

data but were not retained as the final model of free aflibercept according to the statistical criteria.

The next step of modelling was then to add bound aflibercept data, which serves as a marker of efficacy by representing the amount of VEGF bound to aflibercept. The mechanism of action of this drug suggested the use of TMDD model. Among several types, the MM approximation of TMDD model developed by Gibiansky et al proved the most appropriate to reflect the kinetics of aflibercept in our study as free aflibercept concentrations were much higher than target concentrations and their binding to VEGF resulted in a fully saturated target. The relatively low level of free circulating VEGF was confirmed by the range of 19-47 pg/ml of plasma VEGF levels observed in healthy subjects in a meta-analysis [17]. In order to model simultaneously both free and bound drug, the MM equation of bound aflbercept was added into the system of differential equations. Free aflibercept is therefore eliminated through two pathways: non saturable elimination from central compartment (k_{el}) and a specific and saturable binding to VEGF, followed by internalization (k_{int}) of bound aflibercept, which is its dominant elimination pathway. In addition, the formation of bound aflibercept could occur predominantly in central or peripheral compartment. The final PK model was an approximate TMDD model involving two compartments for free aflibercept and one compartment for bound aflibercept, with MM-type binding of free aflibercept to VEGF from the peripheral compartment.

The first-order dissociation rate constant (k_{off}) of the complex to give back free aflibercept was assumed to be negligible. Bound aflibercept might dominantly eliminate by internalization ($k_{int}>>k_{off}$). This assumption is reasonable and consistent with the study of Eppler et al on the development of a TMDD model for recombinant human VEGF (rhVEGF) after i.v. administration in patients with coronary artery disease [18]. VEGF binding to its high affinity

18

receptors was concluded as an essentially irreversible process in vivo. Aflibercept might have the same properties because this drug is produced from two high affinity receptors of aflibercept (VEGFR1 and 2).

Recently, a new derivation of MM approximation of TMDD, called the irreversible binding MM model has been proposed by Gibiansky et al when the dissociation rate constant is negligible and the free target concentration is much smaller than the free drug concentration [19]. The developed model of aflibercept is therefore close to this new approximation of TMDD model. The only difference is that an extra differential equation was added to describe the evolution of bound drug. The MM parameters in the final model represent the combinations of the TMDD model parameters: $V_{\max}=k_{syn}.V_R$ and $K_m=K_{IB}=k_{\deg}/k_{on}$, where V_R is the volume of distribution of target and K_{IB}, k_{syn}, $k_{\deg}$ are the irreversible binding constant, target production rate and target degradation rate, respectively. Although these estimates are not sufficient for the complete description of the full TMDD model, they can provide useful information about the underlying kinetics of drug and target.

During the model development, the general TMDD model with k_{on} and k_{off} was also implemented, assuming that the total target concentration was constant. Free VEGF was then the difference between total VEGF and VEGF in binding to aflibercept. This model showed that k_{on} and k_{off} could not be estimated separately with very small value of k_{off} and its poor precision. Removing k_{off} resulted in the model developed by Epper et al [18], but we obtained unsatisfying fits for bound aflibercept, either for central or peripheral binding to VEGF. A plateau phase after reaching the peak, instead of decreasing phase was predicted for bound aflibercept and the predicted peak was lower.

Alternatively, we also evaluated the linear central or peripheral binding models with a first-order association rate constant (k_{on}) instead of V_{max} and K_m. These models did not describe the observed concentrations of bound aflibercept well, specifically the decreasing phase which illustrate the elimination of bound alibercept after reaching the peak was poorly approached. They were also found less appropriate by statistical criteria.

The nonlinear peripheral binding model was found to better describe the kinetics of drugs than the central binding one, which is consistent with the previous studies on the distribution of VEGF in the body [17]. Large quantities of VEGF were reported in extravascular space of tumour and skeletal muscle [17], suggesting an important source of endogenous VEGF in peripheral compartment and supporting our choice of final model. The plasma concentrations of bound aflibercept in the data were assumed to be the same as those in peripheral compartment, with rapid transfer between extravascular and plasma space.

In the final model, the clearance of bound aflibercept was found to be 6.3 times lower than that of free aflibercept from central compartment (0.14 L/day and 0.88 L/day, respectively). Both free and bound aflibercept eliminate quite slowly. The typical central volume of distribution of free aflibercept was 4.94 L, indicating that free aflibercept has a low level of tissue diffusion and it circulates mostly in the extravascular spaces. The volume of distribution of bound aflibercept was close to that of free aflibercept, which was observed in intermediate models and was fixed to the mean value of V_p in the final model due to the problem of identifiability. In the prior non compartmental analysis of free aflibercept, the average clearance was 0.97 L/day and the steady state volume of distribution was 5.98 L. These values were similar to those estimated by the modelling approach. Compared to a similar antiangiogenic agent, bevacizumab, the central volume of distribution is close but the clearance of total aflibercept is nearly 4 times faster than

20

that of total bevacizumab [20]. From MM parameters, the production rate of VEGF and the irreversible binding constant were calculated to be 0.99 mg/day and 2.91 µg/mL or 19909 pM, respectively. The irreversible binding constant is much larger than the *in vitro* binding affinity K_d observed for VEGF-A. Such a difference is due to the negligible value of k_{off} *in vivo* and it means that the target degradation rate (k_{deg}) is significantly faster than the dissociation rate (k_{off}).

The advantage of this study is the availability of drug concentration data under free and bound forms since they were separately assayed, which is not the case for many antibody products. Generally, only total drug, representing the sum of free and bound was assayed [20-22]. The pharmacokinetic analysis of total form could not provide a good explanation of the mechanism of action of the drug, including the binding to the target; neither was it able to well characterise its pharmacokinetic profile. For example, a simple model of two-compartment infusion with first-order elimination was published for bevacizumab and squalamine, two antiangiogenic agents dosed in total form [20, 21]. The availability of complex data, for aflibercept, helps us characterise both the linear and nonlinear elimination pathways, as well as the complex internalization, and estimate the mechanistic parameters of TMDD system; this could not be achieved using a classical MM model of free drug alone. The concentrations of bound aflibercept could be considered as pharmacodynamic data information of this drug. Our model development was in agreement with the guidelines of modelling for drugs with TMDD properties as mentioned by Yan et al [23]. To our knowledge, the model that we developed is the first mechanism-based population pharmacokinetic model for an anti-VEGF drug.

In conclusion, the present PK model for aflibercept well characterises the underlying mechanism of disposition of aflibercept, where a saturable, high-affinity binding of the aflibercept to its pharmacologic target (VEGF) is responsible for the observed nonlinear pharmacokinetic

behaviour of the free drug. Although further studies will be needed to assess the influence of covariates because of the limited size of the present sample, this model helps to better understand the properties of aflibercept and provides a useful support for further studies in patients during the clinical development, in particular the determination of therapeutic doses using bound aflibercept concentrations as a marker of VEGF inhibition.

APPENDIX: Model development

General peripheral model of target-mediated drug disposition [10,11]:
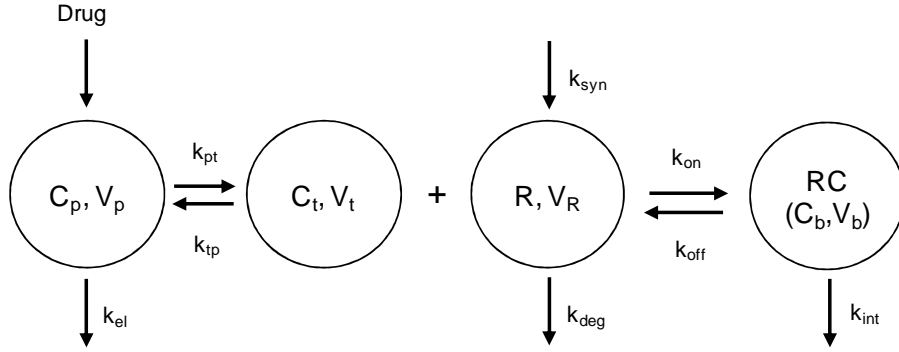
$$\frac{dC_p}{dt} = Input - (k_{el} + k_{pt}).C_p + k_{tp}.\frac{C_t.V_t}{V_p}$$

$$\frac{dC_t}{dt} = k_{pt}.\frac{C_p.V_p}{V_t} - k_{tp}.C_t - \frac{k_{on}.C_t.R.V_R}{V_t} + k_{off}.\frac{C_b.V_b}{V_t} \qquad (A1)$$

$$\frac{dC_b}{dt} = \frac{k_{on}.C_t.R.V_R}{V_b} - k_{int}.C_b - k_{off}.C_b$$

$$\frac{dR}{dt} = k_{syn} - k_{deg}.R - k_{on}.C_t.R + k_{off}.\frac{C_b.V_b}{V_R}$$

where C_p, C_t, C_b, R: the concentrations of free drug in central and peripheral compartment, complex (bound drug) and target; V_p, V_t: volume of distribution of free drug in central and peripheral compartment; V_R, V_b: volume of distribution of target and bound drug in peripheral compartment. k_{el}: elimination rate of free drug from central compartment; k_{on}, k_{off}: association and dissociation rate constant; k_{int}: internalization rate constant of complex; k_{syn}, k_{deg}: target production and degradation rate.

To write this general model, we did not assume that the drug, the target and the bound drug have the same volume of distribution, and we assume that the amount of bound drug created during a unit of time, produced in the compartment of distribution of the target, is $k_{on}.R.C_t.V_R$ [10,11].

When the free drug concentrations are much higher than target concentrations (C>>R) and their binding results in a fully saturated target, the full TMDD can be replaced by the Michaelis-Menten-type (MM) approximations of TMDD model following the suggestions of Gibiansky et al [13,19]. We explain these approximations for peripheral TMDD models.

Approximation 1:

The first MM approximation of TMDD model was proposed in case of reversible binding, basing on the assumptions that the drug-target complex is in a quasi-steady-state or the derivative of the complex concentration, dC_b/dt, is zero [13]. V_R and V_b were assumed to be equal to V_t.

$$k_{on}.C_t.R - (k_{int} + k_{off}).C_b = 0 \tag{A2}$$

$$\frac{C_t.R}{C_b} = \frac{k_{int} + k_{off}}{k_{on}} = K_{ss} \tag{A3}$$

$$C_b = \frac{R_{tot}.C_t}{K_{ss} + C_t} \tag{A4}$$

where R_{tot} is the total concentration of target ($R_{tot}=R+C_b$)

We can rearrange the equation for dC_t/dt, by expressing C_b as a function of C_t and using the expression of K_{ss}, yielding the following equaation:

$$\frac{dC_t}{dt} = k_{pt}.\frac{C_p.V_p}{V_t} - k_{tp}.C_t - \frac{k_{int}.R_{tot}.C_t}{K_{ss} + C_t} \tag{A5}$$

This new equation dC_t/dt therefore includes a Michaelis-Menten-type elimination with

24

$$V_{\max}= R_{tot}. \ k_{\mathrm{int}} \ ; \qquad K_m=K_{ss}=(k_{\mathrm{int}}+k_{off})/k_{on} \qquad\qquad (A6)$$

If, in addition, the total target concentration R_{tot} can be considered constant, $V_{\max}$ is a constant parameter of the system. The TMDD equation system then results in two following equations:

$$\frac{dC_p}{dt} = Input \ - (k_{el} + k_{pt}).C_p + k_{tp}.\frac{C_t.V_t}{V_p}$$

$$\frac{dC_t}{dt} = k_{pt}.\frac{C_p.V_p}{V_t} - k_{tp}.C_t - \frac{V_{\max}.C_t}{K_m + C_t} \qquad\qquad (A7)$$

Approximation 2:

When the binding is irreversible, the dissociation binding rate constant $k_{off}=0$ then the TMDD equations simplify:

$$\frac{dC_p}{dt} = Input \ - (k_{el} + k_{pt}).C_p + k_{tp}.\frac{C_t.V_t}{V_p}$$

$$\frac{dC_t}{dt} = k_{pt}.\frac{C_p.V_p}{V_t} - k_{tp}.C_t - \frac{k_{on}.C_t.R.V_R}{V_t} \qquad\qquad (A8)$$

$$\frac{dC_b}{dt} = \frac{k_{on}.C_t.R.V_R}{V_b} - k_{\mathrm{int}}.C_b$$

$$\frac{dR}{dt} = k_{syn} - k_{\mathrm{deg}}.R - k_{on}.C_t.R$$

The second MM approximation of TMDD models was proposed in the case of irreversible binding. It is based on the assumption that the target is in a quasi-steady-state so that the derivative of target concentration, dR/dt, is zero [19].

$$k_{syn} - k_{\mathrm{deg}}.R - k_{on}.C_t.R = 0 \qquad\qquad (A9)$$

$$R = \frac{k_{syn}}{k_{\mathrm{deg}} + k_{on}.C_t} = \frac{R_0.K_{IB}}{K_{IB} + C_t} \qquad\qquad (A10)$$

25

where K_{IB} is the irreversible binding constant ($K_{IB} = k_{deg} / k_{on}$) and R_0 is the target concentration at baseline ($R_0 = k_{syn}/k_{deg}$), which can be obtained assuming steady-state in the differential equation for R in the absence of drug.

Using this expression for R and noticing that $R_0.K_{IB}.k_{on}=k_{syn}$, we can simplify the equation for dC_t/dt to:

$$\frac{dC_t}{dt} = k_{pt} \cdot \frac{C_p.V_p}{V_t} - k_{tp}.C_t - \frac{1}{V_t} \cdot \frac{k_{syn}.V_R.C_t}{K_{IB} + C_t} \tag{A11}$$

Aslo, generally, only free drug is measured, so that in their model, Gibiansky et al did not take into account the evolution of the complex (dC_b/dt) [19]. The TMDD equation system therefore includes only two equations:

$$\frac{dC_p}{dt} = Input - (k_{el} + k_{pt}).C_p + k_{tp} \cdot \frac{C_t.V_t}{V_p}$$
$$\frac{dC_t}{dt} = k_{pt} \cdot \frac{C_p.V_p}{V_t} - k_{tp}.C_t - \frac{1}{V_t} \cdot \frac{k_{syn}.V_R.C_t}{K_{IB} + C_t} \tag{A12}$$

Application to our study:

In our case, the free aflibercept concentrations were much higher than the target concentrations. We also considered the evolution of bound aflibercept since the concentrations of bound aflibercept were available and could not be considered negligible in the system. In addition, the dissociation rate constant was found to be very small during model development so that irreversible binding and the negligible change in target concentrations (dR/dt) could be assumed, which is similar to the assumptions of the second MM approximation described above. Thus, our differential equation system is (A12) to which we add the equation for dC_b/dt from (A8) where $k_{off}=0$.

26

Substituting the expression for $R = \dfrac{R_0.K_{IB}}{K_{IB} + C_t}$ derived from the second assumption of TMDD

model, we find the following expression:

$$\frac{dC_p}{dt} = Input - (k_{el} + k_{pt}).C_p + k_{tp}.\frac{C_t.V_t}{V_p}$$

$$\frac{dC_t}{dt} = k_{pt}.\frac{C_p.V_p}{V_t} - k_{tp}.C_t - \frac{1}{V_t}.\frac{k_{syn}.V_R.C_t}{K_{IB} + C_t} \qquad (A13)$$

$$\frac{dC_b}{dt} = \frac{1}{V_b}\frac{k_{syn}.V_R.C_t}{K_{IB} + C_t} - k_{int}.C_b$$

Again, we notice a Michaelis-Menten elimination for equation dC_t/dt, which enters the equation of

dC_b/dt as a saturable input.

This equation system can be written with MM parameters, which represents our final model:

$$\frac{dC_p}{dt} = Input - (k_{el} + k_{pt}).C_p + k_{tp}.\frac{C_t.V_t}{V_p}$$

$$\frac{dC_t}{dt} = k_{pt}.\frac{C_p.V_p}{V_t} - k_{tp}.C_t - \frac{1}{V_t}.\frac{V_{max}.C_t}{K_m + C_t} \qquad (A14)$$

$$\frac{dC_b}{dt} = \frac{1}{V_b}.\frac{V_{max}.C_t}{K_m + C_t} - k_{int}.C_b$$

where $V_{max}=k_{syn}.V_R=A_{syn}$ and $K_m= K_{IB}$

For parameter estimation, the micro constants (k_{el}, k_{pt}, k_{tp}) can be replaced by the macro constants:

$Q=k_{tp}.V_t=k_{pt}.V_p$ and $CL=k_{el}.V_p$; where CL is the clearance of free drug from central compartment

and Q is the intercompartment clearance of free drug.

Acknowledgments

List of abbreviations

PK: pharmacokinetics

VEGF: vascular endothelial growth factor

TMDD: target-mediated drug distribution

PlGF: Placental Growth Factor

QE: quasi equilibrium

QSS: quasi steady state

MM: Michaelis-Menten

i.v. : intravenous

s.c. : subcutaneous

LOQ: limit of quantification

GOF: goodness-of-fit

NPDE: normalised prediction distribution error

BQL: below the quantification limit

VPC: visual predictive check

References

1. Baka S, Clamp AR, Jayson GC. A review of the latest clinical compounds to inhibit VEGF in pathological angiogenesis. Expert Opin Ther Targets 2006; 10: 867-76.

2. Folkman J, Merler E, Abernathy C, Williams G. Isolation of a tumor factor responsible for angiogenesis. J Exp Med 1971; 133: 275-88.

3. Holash J, Davis S, Papadopoulos N, Croll SD, Ho L, Russell M, Boland P, Leidich R, Hylton D, Burova E, Ioffe E, Huang T, Radziejewski C, Bailey K, Fandl JP, Daly T, Wiegand SJ, Yancopoulos GD, Rudge JS. VEGF-Trap: a VEGF blocker with potent antitumor effects. Proc Natl Acad Sci U S A 2002; 99: 11393-8.

4. Moreira IS, Fernandes PA, Ramos MJ. Vascular endothelial growth factor (VEGF) inhibition-a critical review. Anticancer Agents Med Chem 2007; 7: 223-45.

5. Salven P, Manpaa H, Orpana A, Alitalo K, Joensuu H. Serum vascular endothelial growth factor is often elevated in disseminated cancer. Clin Cancer Res 1997; 3: 647-51.

6. Ferrara N. Vascular endothelial growth factor: basic science and clinical progress. Endocr Rev 2004; 25: 581-611.

7. Chu QS. Aflibercept (AVE0005): an alternative strategy for inhibiting tumour angiogenesis by vascular endothelial growth factors. Expert Opin Biol Ther 2009; 9: 263-71.

8. Lockhart AC, Rothenberg ML, Dupont J, Cooper W, Chevalier P, Sternas L, Buzenet G, Koehler E, Sosman JA, Schwartz LH, Gultekin DH, Koutcher JA, Donnelly EF, Andal R, Dancy I, Spriggs DR, Tew WP. Phase I study of intravenous vascular endothelial growth factor trap, aflibercept, in patients with advanced solid tumors. J Clin Oncol 2009; 28: 207-14.

9. Sternberg CN. Systemic chemotherapy and new experimental approaches in the treatment of metastatic prostate cancer. Ann Oncol 2008; 19 Suppl 7: vii91-5.

10. Mager DE, Jusko WJ. General pharmacokinetic model for drugs exhibiting target-mediated drug disposition. J Pharmacokinet Pharmacodyn 2001; 28: 507-32.

11. Mager DE. Target-mediated drug disposition and dynamics. Biochem Pharmacol 2006; 72: 1-10.

12. Mager DE, Krzyzanski W. Quasi-equilibrium pharmacokinetic model for drugs exhibiting target-mediated drug disposition. Pharm Res 2005; 22: 1589-96.

13. Gibiansky L, Gibiansky E, Kakkar T, Ma P. Approximations of the target-mediated drug disposition model and identifiability of model parameters. J Pharmacokinet Pharmacodyn 2008; 35: 573-91.

14. Samson A, Lavielle M, Mentre F. Extension of the SAEM algorithm to left-censored data in nonlinear mixed-effects model: Application to HIV dynamics model. Comput Statist Data Anal 2006; 51: 1562-74.

15. Bertrand J, Comets E, Mentre F. Comparison of model-based tests and selection strategies to detect genetic polymorphisms influencing pharmacokinetic parameters. J Biopharm Stat 2008; 18: 1084-102.

16. Brendel K, Comets E, Laffont C, Laveille C, Mentre F. Metrics for external model evaluation with an application to the population pharmacokinetics of gliclazide. Pharm Res 2006; 23: 2036-49.

17. Kut C, Mac Gabhann F, Popel AS. Where is VEGF in the body? A meta-analysis of VEGF distribution in cancer. Br J Cancer 2007; 97: 978-85.

18. Eppler SM, Combs DL, Henry TD, Lopez JJ, Ellis SG, Yi JH, Annex BH, McCluskey ER, Zioncheck TF. A target-mediated model to describe the pharmacokinetics and hemodynamic effects of recombinant human vascular endothelial growth factor in humans. Clin Pharmacol Ther 2002; 72: 20-32.

19. Gibiansky L, Gibiansky E. Target-Mediated Drug Disposition: New Derivation of the Michaelis-Menten Model, and Why It Is Often Sufficient for Description of Drugs with TMDD. PAGE 19, 2010; Abstr 1728 [www.page-meeting.org/?abstract=1728].

20. Lu JF, Bruno R, Eppler S, Novotny W, Lum B, Gaudreault J. Clinical pharmacokinetics of bevacizumab in patients with solid tumors. Cancer Chemother Pharmacol 2008; 62: 779-86.

21. Bhargava P, Marshall JL, Dahut W, Rizvi N, Trocky N, Williams JI, Hait H, Song S, Holroyd KJ, Hawkins MJ. A phase I and pharmacokinetic study of squalamine, a novel antiangiogenic agent, in patients with advanced cancers. Clin Cancer Res 2001; 7: 3912-9.

22. Hayashi N, Tsukamoto Y, Sallas WM, Lowe PJ. A mechanism-based binding model for the population pharmacokinetics and pharmacodynamics of omalizumab. Br J Clin Pharmacol 2007; 63: 548-61.

23. Yan X, Mager DE, Krzyzanski W. Selection between Michaelis-Menten and target-mediated drug disposition pharmacokinetic models. J Pharmacokinet Pharmacodyn 2010; 37: 25-47.

Table 1-Parameter estimates for the best free and bound model

Fixed effects		Interindividual variability	Residual variability		
Parameter	Estimate (RSE%)	ω (%) (RSE%)		σ_a (µg/mL) (RSE%)	σ_p(%) (RSE%)
CL (L/day)	0.88 (4.0)	28.0 (10)	Free aflibercerpt	0.05 (9.0)	17.1(3.0)
V_p (L)	4.94 (4.0)	27.3 (10)	Bound aflibercept	-	12.6 (4.0)
Q (L/day)	1.39 (9.0)	49.8 (14)			
V_t (L)	2.33 (7.0)	39.8 (14)			
V_b (L)	4.94 (=V_p)	-			
V_{max} (mg/day)	0.99 (5.0)	13.6 (17)			
K_m (µg/mL)	2.91 (11)	45.6 (15			
k_{int} (day^{-1})	0.028 (5.0)	-			

CL: Clearance of free aflibercept from central compartment ($CL=k_{el}.V_p$)

Q: Intercompartment clearance of free aflibercept ($Q=k_{tp}.V_t=k_{pt}.V_p$)

Figure legends

Figure 1

Observed concentrations of free aflibercept (µg/mL) and bound aflibercept (µg.eq/mL) versus time.

Figure 2

Proposed structural models for free and bound aflibercept (2 compartments for free aflibercept, 1 compartment for bound aflibercept) with binding to VEGF occurring in the peripheral compartment.

Figure 3

Diagnostic goodness-of-fit plots for the model of free and bound aflibercept, showing observed versus population predicted concentrations (PRED), observed versus individual predicted concentrations (IPRED) and normalized prediction distribution error (NPDE) versus population predicted concentrations. The lower limit of quantification for bound aflibercept was 43.9 ng/mL (0.0314 µg.eq/mL). BQL observations were removed from the plots.

Figure 4

Examples of individual fits for 4 representative individuals. From left to right: study 1 with dose of 2 mg/kg, study 2 with dose of 1, 2, 4 mg/kg. Fits for free aflibercept are presented in the top, bound afibercept in the middle, and the first 24h fits of bound aflibercept in the bottom. Observed data are plotted using a circle (∘) and BQL data are plotted using a star (*). The line (−) represents the prediction of model.

Figure 5

Visual predictive check (VPC) of free aflibercept in semi-logarithmic scale (top), and bound afibercept in linear scale (bottom) for the final model. Observed data are plotted using a solid circle (•) and censored data are plotted using a star (*). The shaded area and the dotted lines represent the 90% prediction interval and the predicted median of 10th, 50th and 90th percentiles of simulated data (n=500). The solid lines represent the 10th, 50th and 90th percentiles of observed data.
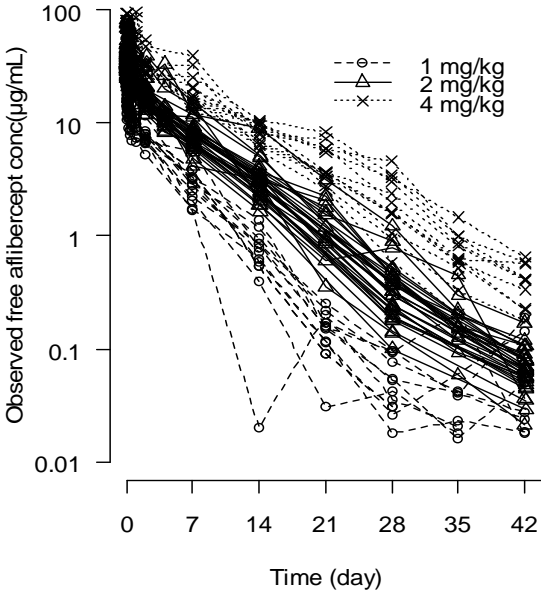
Figures

Figure 1

Figure 2

Infusion

Plasma free aflibercept C_p, V_p k_{pt} Tissue free aflibercept C_t, V_t V_{max}, K_m Bound aflibercept C_b, V_b
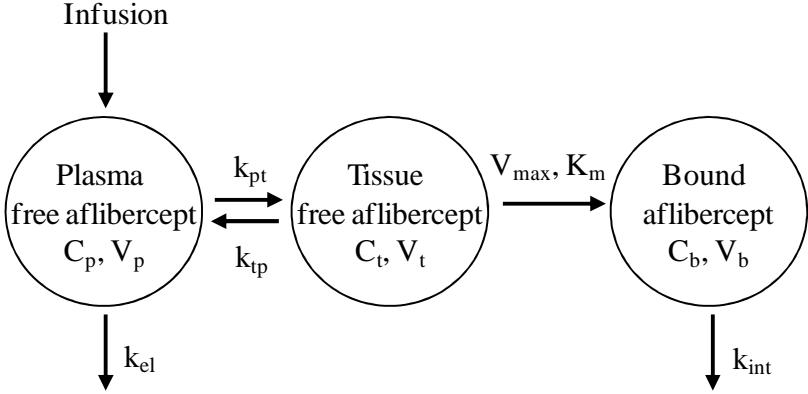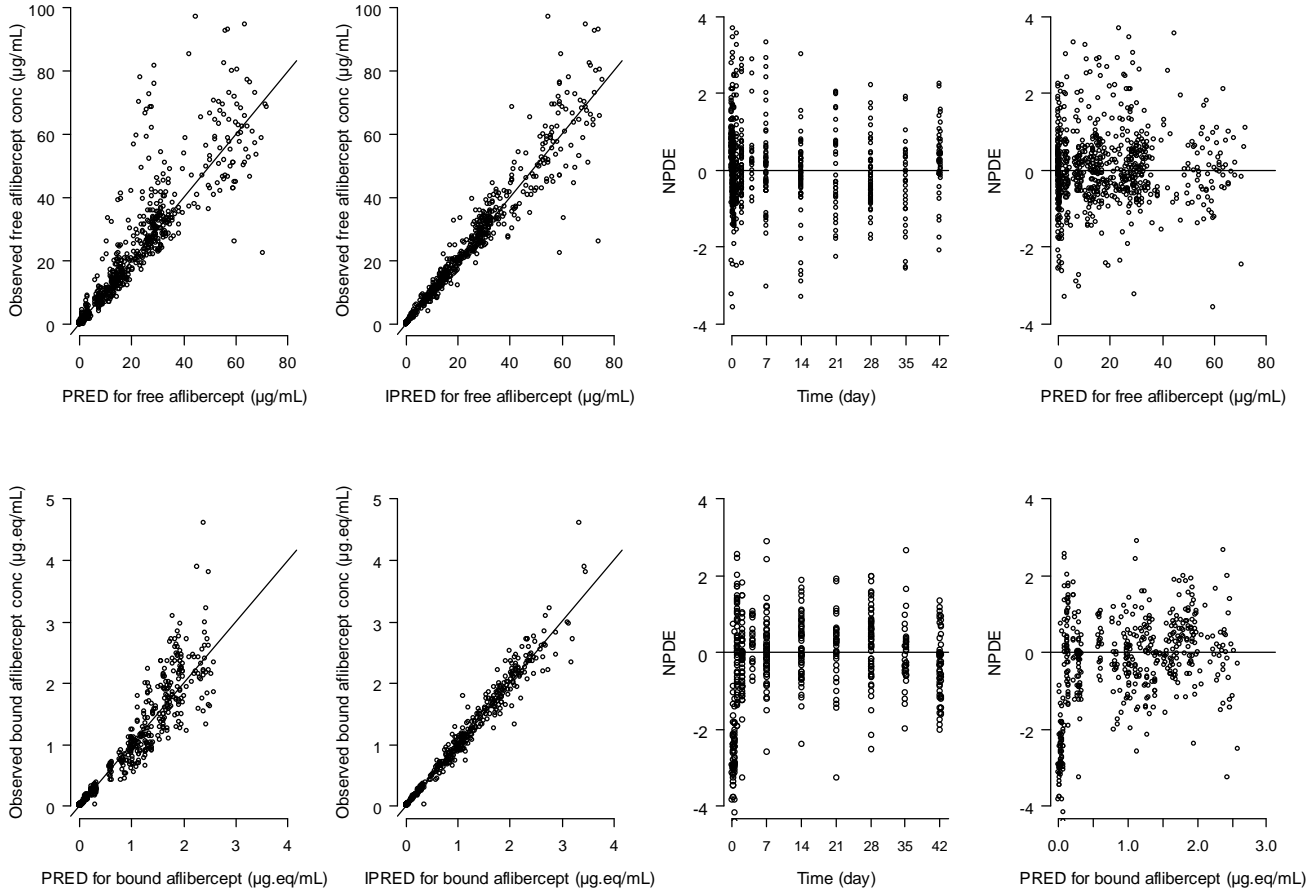
k_{tp}

k_{el}

k_{int}
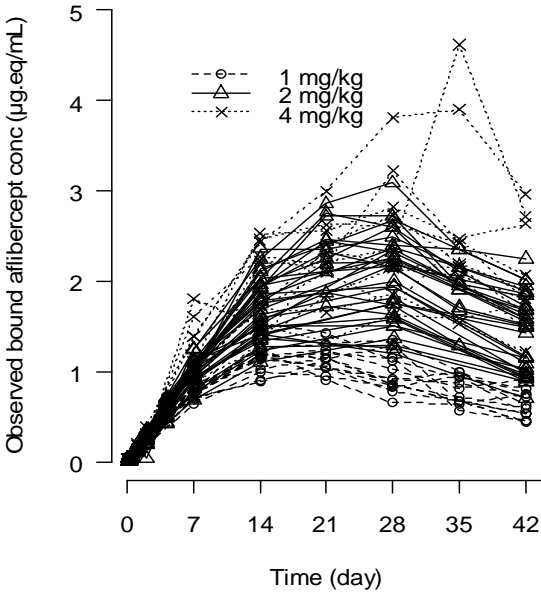
Figure 3

Figure 4

Figure 5